Topology of NGEP, a Prostate-Specific Cell:Cell Junction Protein Widely Expressed in Many Cancers of Different Grade Level

Sudipto Das,[1] Yoonsoo Hahn,[1] Dawn A. Walker,[1] Satoshi Nagata,[1] Mark C. Willingham,[2] Donna M. Peehl,[3] Tapan K. Bera,[1] Byungkook Lee,[1] and Ira Pastan[1]

[1]Laboratory of Molecular Biology, Center for Cancer Research, National Cancer Institute, NIH, Bethesda, Maryland; [2]Department of Pathology, Wake Forest University School of Medicine, Winston-Salem, North Carolina; and [3]Department of Urology, Stanford University School of Medicine, Stanford, California

Abstract

New gene expressed in prostate (NGEP) is a prostate-specific polytopic membrane protein found at high concentrations at cell:cell contact regions. To determine if NGEP is a useful target for antibody-based therapy of prostate cancer, we performed an immunohistochemical analysis of 126 human prostate carcinoma samples using polyclonal anti-NGEP sera and found that 91% of the cancers express NGEP protein. To elucidate the topology of NGEP and guide the development of monoclonal antibodies (mAb) reacting with the extracellular regions of NGEP, a hemagglutinin epitope tag was inserted at several positions within the NGEP sequence. The tagged proteins were expressed in 293T cells and locations of the tags were determined by immunofluorescence in intact or permeabilized cells. The results indicate that NGEP contains eight transmembrane domains with both the NH_2 and COOH termini of NGEP located inside the cell. We produced mAb to three regions that are predicted to be intracellular based on the epitope tag data (amino acids 1-352, 441-501, and 868-933), and as predicted, the mAb only detected the protein in permeabilized cells. NGEP is a glycoprotein with predicted glycosylation sites at N809 and N824. When these residues were converted to glutamine, glycosylation was abolished, confirming that the residues are extracellular. Our findings on the expression and the orientation of the NGEP protein serve as an important framework for the development of mAb targeting the extracellular regions of NGEP that could be used for prostate cancer immunotherapy. [Cancer Res 2008;68(15):6306–12]

Introduction

Prostate cancer is one of the leading causes of cancer deaths among men (1). It is predicted that approximately one in six men in the United States will have prostate cancer in their lifetime (2). Currently, the most common treatment regimen is surgery followed by radiation or radiation paired with hormone therapy (3–5). However, the current treatments are highly unsuccessful if the cancer has undergone metastasis or in cases of hormone-independent prostate cancer (6). Recently, clinical trials using monoclonal antibodies (mAb) against cell surface receptors have yielded encouraging therapeutic results on both lymphomas and solid tumors (7, 8). New gene expressed in prostate (NGEP) is a promising target for therapeutic antibody for prostate cancer because it is only expressed in normal prostate (not essential) and prostate cancer (9) and not in any other vital organs. In addition, its cell surface expression makes NGEP an excellent immunotherapeutic target.

NGEP, a TMEM16 protein family member, is a polytopic plasma membrane protein highly concentrated at cell:cell contact regions in LNCaP cells (10). Immunohistochemistry of prostate tissues showed that NGEP is highly expressed on the apical and lateral surfaces of normal prostate and prostate cancer cells (10). Lateral surface expression suggests that NGEP may have a role in prostate cell interactions or adhesions. Furthermore, LNCaP cells expressing NGEP formed aggregates as the cell density increases. This phenomenon of aggregation was lost when a small interfering RNA targeting NGEP mRNA was introduced into the NGEP-expressing LNCaP cells (10).

Experimental validation of the predicted topological structure of NGEP is important to understand the structural basis of its action and for the development of novel therapeutic antibodies against its extracellular region for prostate cancer immunotherapy. Several *in silico* analysis programs have proposed different topological models of NGEP. For example, the hydropathy analysis of the amino acid sequence using the Kyte and Doolittle algorithm predicted that NGEP will have seven transmembrane regions, whereas PredictProtein analysis predicted that NGEP will have eight transmembrane regions (11, 12). To experimentally determine the topology of NGEP, we used an epitope tag insertion scanning method (13, 14).

In this study, the hemagglutinin (HA) epitope was incorporated in all predicted extracellular and intracellular regions of the protein. The epitope insertion constructs were transfected into 293T cells and their accessibility to the antiepitope antibodies was evaluated in permeabilized and intact cells to determine their orientation relative to the plasma membrane. Further, we developed and characterized mAbs that are specific to NGEP. Using these antibodies in combination with *N*-glycosylation analysis of NGEP, we confirmed our predicted model obtained from the epitope insertion studies. Our results indicate that NGEP consists of eight transmembrane regions with both the NH_2 and COOH termini being intracellular. In addition, our results suggest that a hydrophobic region within extracellular loop 3 between TM5 and TM7 protrudes into the membrane forming a reentrant loop-like structure. This experimentally verified membrane topology

Note: Supplementary data for this article are available at Cancer Research Online (http://cancerres.aacrjournals.org/).

Current address for Y. Hahn: Department of Life Science, College of Natural Science, Chung-Ang University, Seoul 156-756, Korea. Current address for S. Nagata: Cancer Biology Research Center, Sanford Research/University of South Dakota, 1400 West 22nd Street, Sioux Falls, SD 57105.

Requests for reprints: Ira Pastan, Laboratory of Molecular Biology, National Cancer Institute, 37 Convent Drive, Room 5106, Bethesda, MD 20892-4264. Phone: 301-496-4797; Fax: 301-402-1344; E-mail: pastani@mail.nih.gov.

doi:10.1158/0008-5472.CAN-08-0870

structure of NGEP should permit us to develop novel therapeutic antibodies specific to the extracellular region of NGEP for prostate immunotherapy.

Materials and Methods

Bioinformatic identification of NGEP paralogs and orthologs. To make a NGEP topology model by using information of paralogs and orthologs in various mammalian species, we searched the genome sequence database of different species with the *NGEP* cDNA as a query. The putative NGEP genomic sequence was extracted from each genome assembly. We then identified each exon from the genomic sequence by comparing it with human NGEP exons. Finally, the exons were assembled into a virtual cDNA sequence. The resulting sequences were checked using expressed sequence tags (EST) when available. We successfully identified complete or nearly complete NGEP/Ngep protein sequences from chimpanzee (*Pan troglodytes*), rhesus macaque (*Macaca mulatta*), mouse (*Mus musculus*), rat (*Rattus norvegicus*), and dog (*Canis familiaris*). The predicted mouse and rat *Ngep* cDNA sequences are available in Genbank (accession numbers BK004075 and BK004074, respectively).

Construction of membrane topology models of human NGEP. To predict a possible membrane topology of the human NGEP protein, we used the transmembrane domain prediction program TMAP (15). As inputs, we prepared two multiple sequence alignments: one with selected mammalian NGEP orthologs (human, rhesus macaque, mouse, rat, and dog) and the other with selected human paralogs (NGEP, TMEM16A, TMEM16B, TMEM16C, TMEM16D, TMEM16E, TMEM16F, and TMEM16J) using ClustalX (16).

DNA constructs. Epitope-tagged EGFP-NGEP at discrete locations (Supplementary Table S1) was generated by the introduction of a 9–amino acid peptide (YPYDVPDYA) representing the HA of influenza virus into EGFP-NGEP cDNA by PCR mutagenesis (17). A full-length cDNA for NGEP cloned into pEGFP-C1 (Clontech) was used as a template for the insertional mutagenesis. The HA insertion was verified by DNA sequencing.

Immunohistochemistry. Paraffin-embedded prostate tissue samples, provided by D.M.P. from archival, formalin-fixed radical prostatectomy specimens from Stanford University School of Medicine (the Office of Human Subjects Research, NIH, has designated these samples exempt), were cut into 5-μm sections. Immunohistochemistry was performed by Histoserv, Inc. as previously described (10). Each immunostained tissue section was assessed by a single pathologist, and the staining intensity in normal and tumor cells in the same tissue section was scored on an arbitrary scale of 0 to 3 (3 indicates strong NGEP staining and 0 being no reaction).

Immunofluorescence and confocal microscopy. The 293T cells were obtained from the American Type Culture Collection and grown in DMEM containing 10% fetal bovine serum and a penicillin (100 units/mL)/streptomycin (100 μg/mL) mixture at 37°C in a humidified atmosphere with 5% CO_2. For immunofluorescence experiments, 293T cells were grown on poly-lysine–coated coverslips. Transfection of the EGFP-NGEP epitope-tagged constructs was performed using Lipofectamine 2000 (Invitrogen) according to the manufacturer's instructions. Forty-eight hours after transfection, the cells were washed with Dulbecco's PBS (DPBS) and fixed with 3.7% formaldehyde at room temperature for 10 min. Nonpermeabilized cells were washed thrice with DPBS and then blocked with 10% normal goat serum for 30 min. Subsequently, the cells were incubated with a monoclonal HA antibody (1:500; Covance) for 1 h followed by three washes and incubated with goat anti-mouse conjugated with Alexa Fluor 546 (Invitrogen) at 2 μg/mL concentration in blocking buffer for 45 min. The cells were washed with DPBS and then stained with Hoechst 33342 (1:500; Invitrogen) for 15 min, mounted in ProLong Gold Antifade reagent (Invitrogen), and examined using a Zeiss 510 inverted laser scanning microscope. For immunofluorescence under permeabilized conditions, the cells were permeabilized with 0.1% Triton X-100 in DPBS for 10 min after fixation. The steps following were the same as performed for the nonpermeabilized cells.

Subcellular fractionation and deglycosylation. MCF7 cells stably transfected with NGEP were used for subcellular fractionation. Subconfluent

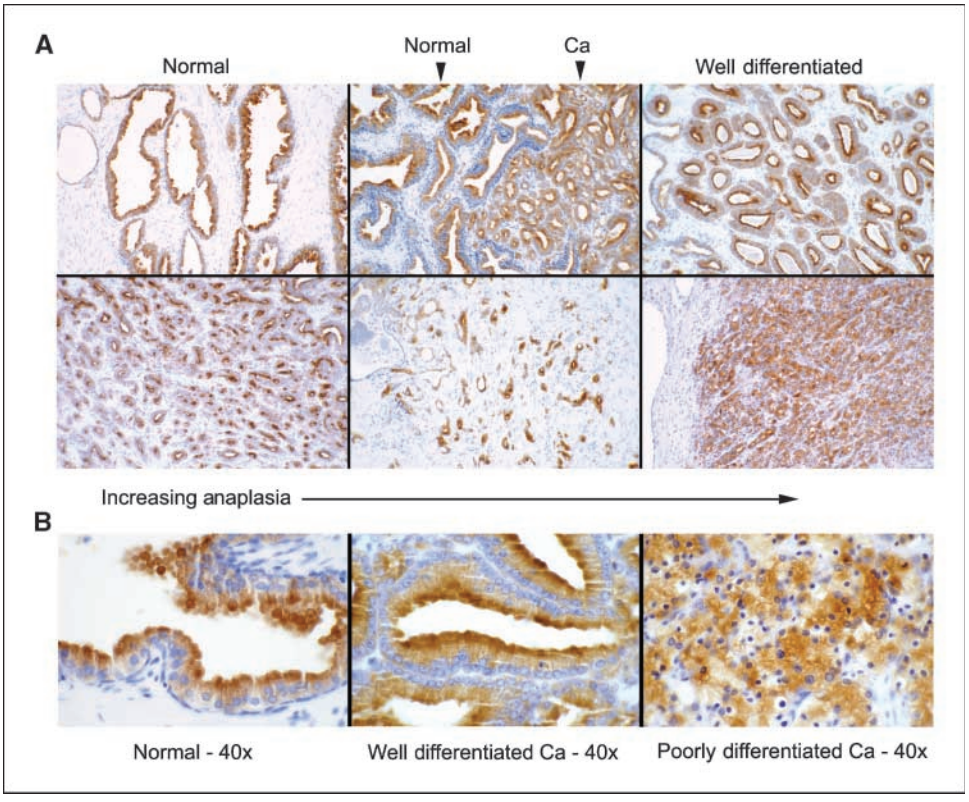

Figure 1. Immunohistochemical staining of NGEP in prostate cancer tissues. *A,* representative examples of NGEP staining shown at low magnification (×10) ranging from almost normal-looking acini to less-organized or disorganized prostate cancer cells. *Arrows,* normal and cancer (*Ca*) cells. *B,* NGEP staining at higher magnification (×40) showing the apical localization of NGEP.

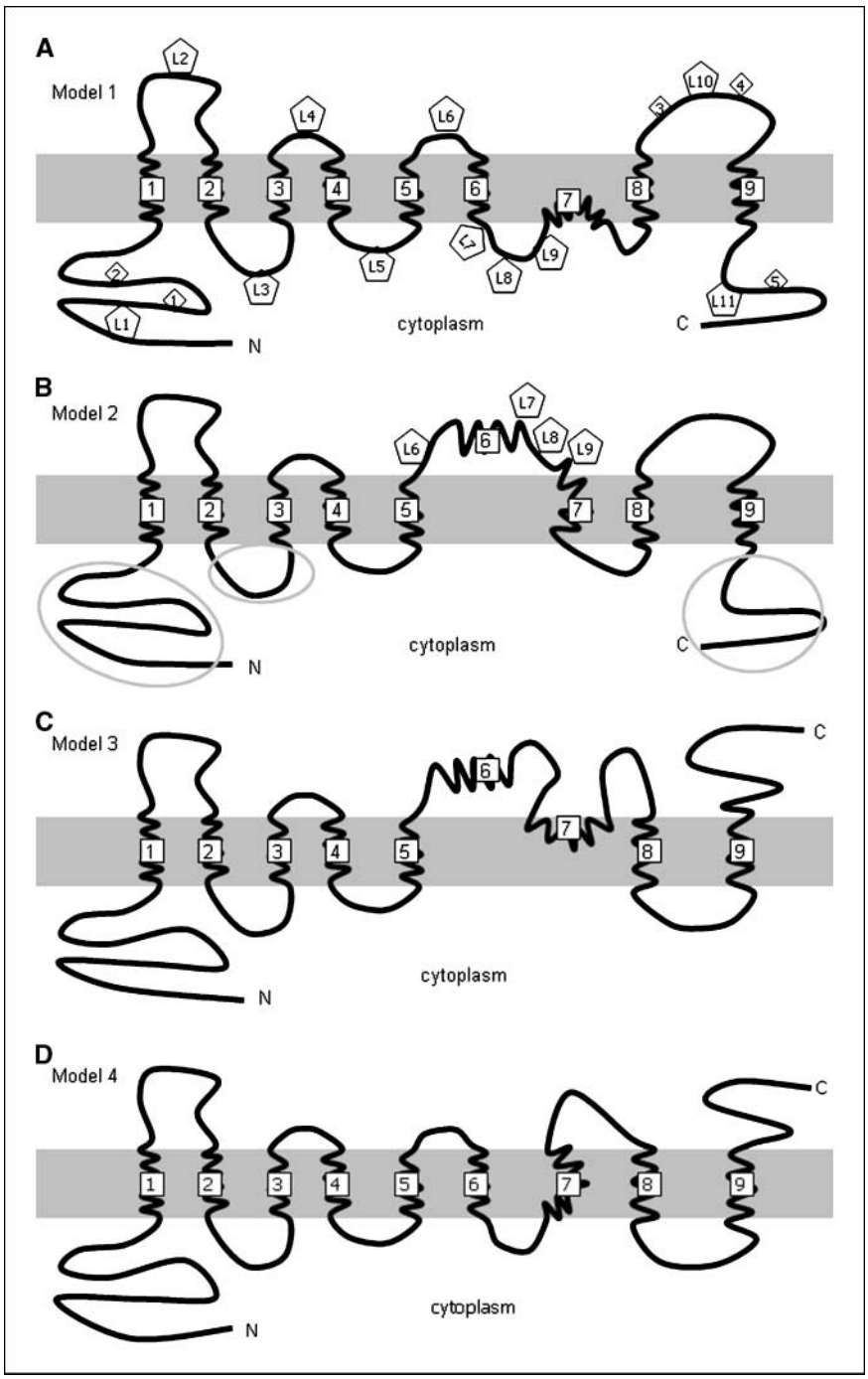

Figure 2. Possible membrane topologies of NGEP. The four possible membrane topologies of NGEP are depicted. The predicted transmembrane domains are numbered 1 to 9. In model 1 (*A*) and model 2 (*B*), both the NH_2 and COOH termini are intracellular, whereas in case of model 3 (*C*) and model 4 (*D*) the NH_2 and COOH termini are intracellular and extracellular, respectively. *A,* the predicted *N*-glycosylation sites are shown as numbered diamonds in model 1. The HA insertion sites are shown as numbered pentagons in models 1 (*A*) and 2 (*B*). *B,* the NGEP fragments against which the mAbs were raised are circled in model 2.

cells were scraped after washing with PBS and centrifuged at 200 × *g* for 5 min. The cell pellet was resuspended with buffer containing 10 mmol/L KCl, 1.5 mmol/L $MgCl_2$, and 10 mmol/L Tris-HCl (pH 7.5) supplemented with protease inhibitors (Sigma) and 0.5 mmol/L DTT. After incubation on ice for 5 min, the swollen cells were broken open with 20 strokes of a Dounce homogenizer. The homogenate was centrifuged at 1,000 × *g* for 10 min to pellet the nuclear fraction. The supernatant was centrifuged at 100,000 × *g* for 1 h and the pellet was designated as the membrane fraction. For deglycosylation, 40 μg of the membrane fraction were solubilized and denatured in 30 mL of 0.2 mol/L NaH_2PO_4 (pH 8.6), 0.5% (v/v) β-mercaptoethanol, 0.1% SDS, 0.25 mmol/L phenylmethylsulfonyl fluoride (PMSF), and 1.25 mmol/L Tris-Cl and incubated for 10 min. Subsequently, 30 mL of 1.25% (v/v) NP40, 0.4 μg/mL bovine serum albumin, 20 mmol/L EDTA, 4 μg/mL leupeptin, 2 μg/mL pepstatin, 4 μg/mL aprotinin, and 1 mmol/L PMSF were added. The mixture was then divided into two equal aliquots. To one of these samples, 2 μL of PNGaseF (New England Biolabs) were added. Parallel samples (with or without PNGaseF) were incubated overnight at 30°C and analyzed by immunoblot.

Production of the mAbs. Mice were immunized with a fusion protein between the NGEP fragment and GST, expressed as inclusion bodies in *Escherichia coli* GC5 (GeneChoice). The characteristics of the mAbs are shown in Supplementary Table S2. All the mAbs reacted with the specific NGEP fragment used for immunization and showed no cross-reactivity with the other two NGEP fragments.

Western blotting. The 6x-His-NGEP fusion proteins (10 ng) and 20 μg of cell lysate were separated on 4% to 20% SDS-polyacrylamide gels (Invitrogen) under reducing conditions. Transfer of the proteins to polyvinylidene difluoride membrane (Invitrogen) and immunostaining with mAbs or polyclonal antibodies were carried out as previously described (18).

Results

NGEP expression analysis on prostate cancer specimens. To investigate if NGEP is expressed in a wide variety of prostate cancer specimens, we performed immunohistochemistry using a polyclonal antibody raised against the COOH terminus of NGEP on 126 prostate specimens from men who had undergone radical prostatectomy. The specimens had been subjected to a complete histologic review and each tissue section had normal/benign glands along with cancerous regions represented by Gleason grade 3, 4, or 5. NGEP was detected in 100% of the normal region of specimen, with an average intensity of 2.5. Ninety-one percent of the specimens were positive for NGEP in the cancerous region with an average intensity of 1.8. The average intensity of NGEP expression with respect to the grade level of prostate cancer did not change with respect to the grade level (Supplementary Table S3). To test the cross-reactivity of the polyclonal antibody, we performed immunohistochemistry using several normal tissues: kidney, liver, stomach, brain, heart, lung, and prostate. None of the tissue samples, except the prostate, showed a signal, indicating that the polyclonal antibody is specific to NGEP (data not shown). NGEP expression was also found positive in prostate tumors metastasized to lymph nodes (data not shown). Examples of the NGEP immunostaining at lower magnification (×10) with respect to the anaplasia are illustrated in Fig. 1*A*. Higher magnification images (×40) of NGEP immunostaining show that the apical staining of NGEP is similar for both normal and well-differentiated prostate cancer (Fig. 1*B*). In case of the poorly differentiated cancer specimens, the glandular structure is less obvious, but NGEP is present in the membrane (Fig. 1*B, right*). These results indicate that NGEP is widely expressed from well-differentiated to poorly differentiated prostate cancer and suggest that NGEP could be an excellent target for antibody-based immunotherapy.

Models of the membrane topology of human NGEP protein. NGEP was identified as a prostate-specific polytopic protein. To locate the transmembrane domains and infer the membrane topology of the human NGEP protein, we predicted transmembrane

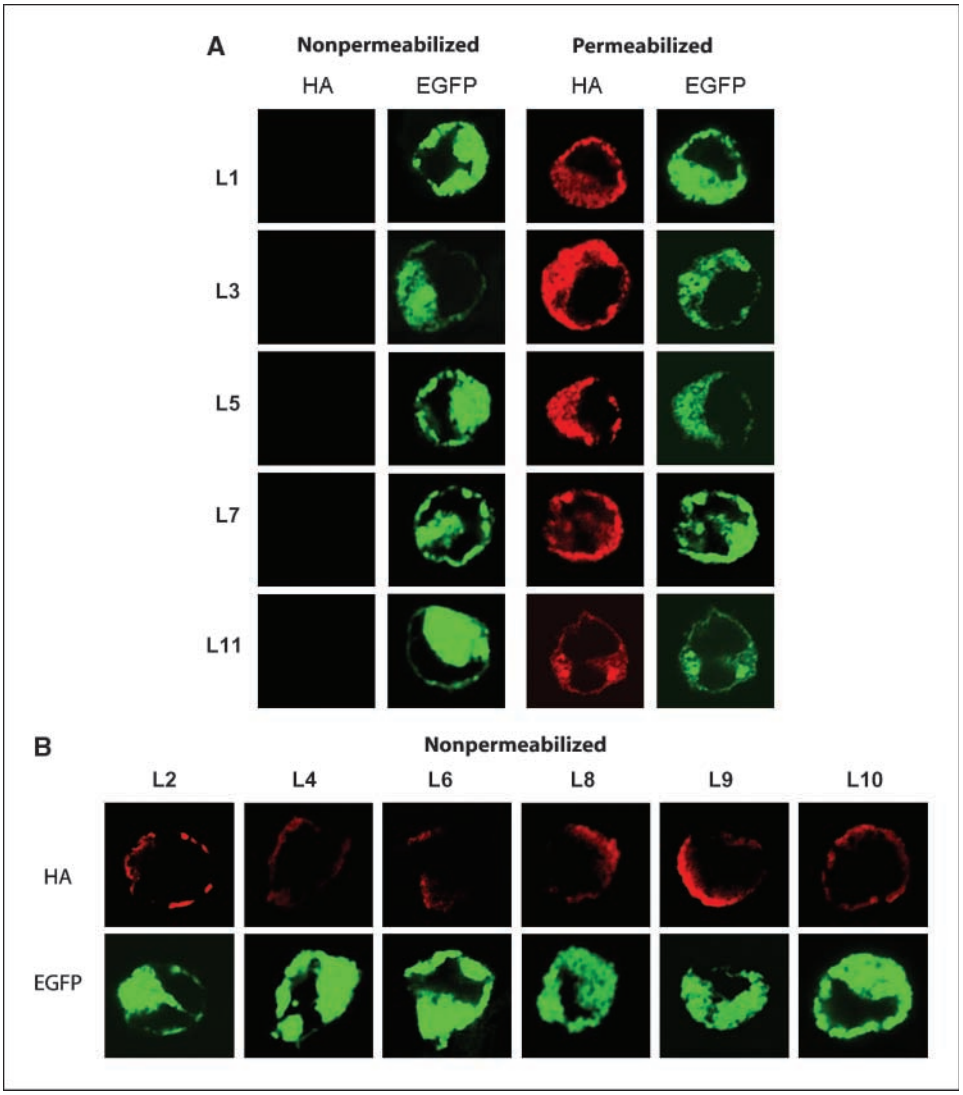

Figure 3. Detection of the HA-tagged EGFP-NGEP mutants by immunofluorescence. The 293T cells were transfected with the HA-tagged insertion mutants, and 24 h after transfection, the cells were processed for immunofluorescence in both nonpermeabilized and permeabilized conditions. The expression of the proteins was detected by using anti-HA mAb and the signal was detected using Alexa Fluor 546–labeled goat anti-mouse antibody. The tagged mutants were then categorized according to their apparent intracellular (*A*) or extracellular (*B*) localizations.

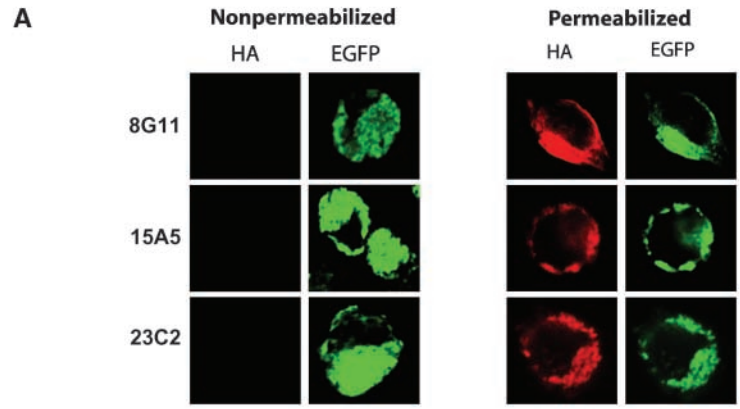

B

NGEP antibody	NGEP region	Immunofluorescence		HA insertion	Construct	Immunofluorescence	
		Permeabilized	Nonpermeabilized			Permeabilized	Nonpermeabilized
8G11	1-352	+	-	117-118	L1	+	-
15A5	441-501	+	-	461-462	L3	+	-
23C2	868-933	+	-	907-908	L11	+	-

Figure 4. Reactivity of anti-NGEP antibodies to NGEP. *A,* confocal images of 293T cells transfected with EGFP-NGEP and the resulting immunofluorescence measured under permeabilized and nonpermeabilized conditions using the mAb raised against NGEP. The 293T cells were transfected with EGFP-NGEP and the expression of the NGEP was detected by the mAb raised against NGEP. The signal was detected using Alexa Fluor 546–labeled goat anti-mouse antibody. *B,* comparison of the immunofluorescence signal obtained from the mAb derived against NGEP and with the epitope insertion constructs.

domains of the human NGEP paralogs and the mammalian orthologs by using the TMAP prediction program. The TMAP program predicted nine transmembrane domains (referred to as TM1 to TM9 hereafter) from the alignment of eight human NGEP paralogs (Supplementary Table S4; Supplementary Fig. S1). It predicted eight transmembrane domains from the alignment of five NGEP orthologs; TM6 was not present in the predicted topology. Interestingly, TM7 contains two conserved prolines within the predicted transmembrane helix. It has been reported that proline residues in helices induce kinks (19, 20). Hence, we speculated that TM7 might form a sharp bend or reentrant loop (21) owing to the two prolines. Incorporating the uncertainty of TM6 and TM7, we developed four alternative models for the membrane topology of human NGEP (Fig. 2). Based on these predictions, the NH_2 terminus of NGEP is proposed to be localized intracellularly in all of the models, whereas the COOH terminus is intracellular in two of the four models.

Determination of the topology of NGEP. To experimentally determine the cellular location of the NH_2 and COOH termini of NGEP, we inserted a HA epitope between hydrophilic residues outside the putative transmembrane domains (Supplementary Table S1). The 293T cells were chosen as the cell line for transfection, as NGEP is present both in the plasma membrane and in the intracellular membranes as reported previously (10). An EGFP-NGEP fusion protein was used so that the dual fluorescence from EGFP and the HA epitope antibody could confirm the membrane orientation of NGEP and serve as an internal control within the same cell. Immunofluorescence was performed under permeabilized and nonpermeabilized conditions and the results indicate the NH_2 terminus of NGEP is located in the cytosol. Immunofluorescence signal was not observed with the construct L1 (Fig. 2*A*; Supplementary Table S1) in nonpermeabilized cells (Fig. 3*A*). We observed immunofluorescence along the periphery of the cell and at the intracellular membrane only after treatment with the permeabilization agent (Fig. 3*A*). This anti-HA signal colocalizes with the fluorescence from the EGFP-NGEP fusion protein. The L11 construct carries a HA tag near the COOH terminus (Supplementary Table S1). Immunostaining is only observed under permeabilized conditions (Fig. 3*A*). These results indicate that both the NH_2 and COOH termini of NGEP are intracellular and the topology of NGEP could be either model 1 (Fig. 2*A*) or model 2 (Fig. 2*B*). Model 3 (Fig. 2*C*) and model 4 (Fig. 2*D*) predict the COOH terminus to be extracellular, which does not agree with our findings.

To further verify that NGEP has the topology of models 1 or 2, an epitope tag (L10) was inserted between TM8 and TM9 (Fig. 2). This epitope is predicted to be extracellular in case of models 1 and 2, whereas it is predicted to be intracellular in case of models 3 and 4. In 293T cells expressing construct L10, red fluorescence was detected in the absence (Fig. 3*B*) and in the presence of the permeabilizing agent (data not shown), indicating the extracellular location of this region. This further agrees with the location found in models 1 or 2.

To differentiate between models 1 and 2, four epitope tags (L6, L7, L8, and L9) were inserted between TM5 and TM7. According to model 1, L6 would be on the cell surface, whereas L7, L8, and L9 should be intracellular. In contrast, L6, L7, L8, and L9 are predicted to be extracellular according to model 2. In 293T cells expressing constructs L6, L8, and L9, the HA epitope was accessible under nonpermeabilized conditions, indicating the extracellular location of these epitopes (Fig. 3*B*), whereas in the case of L7 the HA epitope was accessible only when the cells were permeabilized, indicating the intracellular location of this epitope (Fig. 3*A*). These results show that neither model 1 nor model 2 represents the correct topology of NGEP.

To further verify the orientation of the extracellular and the intracellular loops between TM1 and TM5, epitope tags were inserted in various locations and immunofluorescence was performed under permeabilized and nonpermeabilized conditions. In 293T cells expressing construct L2 and L4, red fluorescence was detected in the absence of permeabilizing agent (Fig. 3*B*), indicating the extracellular location of these regions. In 293T cells

expressing constructs L3 and L5, the HA epitope was accessible only when the cells were permeabilized, indicating the intracellular location of these epitopes (Fig. 3*A*).

Validation of the topology. As the epitope insertion method bears the risk of changing the topogenic activity of the neighboring membrane-spanning domains, we confirmed the topology of NGEP by (*a*) immunofluorescence using mAb against specific regions of NGEP and (*b*) analyzing the *N*-glycosylation sites of NGEP.

EGFP-NGEP was transfected into 293T cells and the mAbs (Fig. 2*B*; Supplementary Table S2) were used to determine the cellular location of the antigenic sites by immunofluorescence staining with or without cellular membrane permeabilization. Only under permeabilized conditions were all of the three mAbs able to detect NGEP (red fluorescence), which colocalizes with EGFP-NGEP (green fluorescence; Fig. 4*A*), showing that the antigenic regions are cytosolic. The results obtained from the mAb are consistent with the HA epitope insertion experiments as shown in comparative results in Fig. 4*B*. In construct L1 (HA epitope inserted between amino acid 117 and 118), HA antibody could assess the epitope only when the cells were permeabilized (Fig. 3*A*). Similarly, the mAb 8G11 raised against NGEP amino acid 1-352 could detect NGEP only in the permeabilized cells and not in the nonpermeabilized conditions (Fig. 4*A*). Similar results were obtained from construct L3, antibody 15A5, and also construct L11 and 23C2.

Using bioinformatic analysis, we predicted possible *N*-glycosylation sites [Asn-Xaa-(Ser/Thr) motifs] in NGEP. The predicted *N*-glycosylation sites are shown in Fig. 2*A*. The *N*-glycosylation sites N164 (site 1), N201 (site 2), and N904 (site 5) are present in the NH_2 and COOH termini of NGEP, which based on both the L1 and L11 HA tag experiments and the mAbs (8G11 and 23C2) reported above are predicted to be cytosolic, making these sites unlikely to be glycosylated. The other two predicted *N*-glycosylation sites, N809 (site 3) and N824 (site 4), present in the extracellular loop between TM8 and TM9 could be *N*-glycosylation sites. To assess whether N809 and N824 are glycosylated, we analyzed the membrane fraction of MCF7 cells stably transfected with NGEP. The crude membrane fraction of NGEP-transfected MCF7 cells was isolated and immunoblotted with a NGEP polyclonal antibody raised against the COOH terminus of NGEP (10). The crude membrane fraction of the MCF7 cells expressing NGEP showed a predicted 100-kDa band and also an additional band with an apparent molecular weight of ~120 kDa. This 120-kDa band disappeared after treatment with PNGaseF (Fig. 5). When the putative *N*-glycosylation sites were removed by mutating the asparagine at position 809 and 824 to a glutamine (N809Q/N824Q), the 120-kDa band did not appear (Fig. 5) and PNGaseF did not affect the migration pattern of the NGEP. These data indicate that N809 and N824 are glycosylated and thus must be located on an extracellular surface. This finding agrees with our finding that the tag between TM8 and TM9 (construct L10) is present in the extracellular surface of the cell (Fig. 3*B*).

Discussion

Targeting cancer cells with mAbs has become an indispensable component of modern treatment against solid tumors, such as prostate and breast cancer (7, 8). For this therapy to be effective, it is essential that the antigen is expressed on the cell surface of the target cells and not expressed in essential normal tissues, such as brain, liver, heart, kidney, stomach, lung, and pancreas. NGEP, identified through computer-based analysis of EST clustering, is a prostate-specific plasma membrane protein (9).

In the present study, we have determined the topological structure of NGEP. A computational analysis of NGEP topology using the TMAP prediction program predicted seven to nine transmembrane domains with four possible topologies (Fig. 2). To experimentally determine the topology, we used epitope tag insertion scanning mutagenesis to strategically insert epitope tags into discrete regions of NGEP. The modified proteins were expressed in 293T cells and the accessibility of the HA epitope was determined in both intact and permeabilized cells. All of the constructs were expressed in the plasma membrane with an intracellular accumulation of NGEP as a result of overexpression. Based on our study, we propose an 8TM topology model of NGEP in which both the NH_2 and COOH termini are cytosolic. This model is quite similar to model 2 made by the TMAP prediction program but has one difference (Fig. 2*B*). The extracellular loop 3, between TM5 and TM7 (containing one hydrophobic segment, amino acids 628-657), predicted to be extracellular in model 2, protrudes partially into the membrane and forms a reentrant loop structure between TM5 and TM7. We suggest this model because no immunofluorescence signal was observed in nonpermeabilized cells when L7 was transfected into 293T cells (Figs. 3*A* and 6). This type of structure is found in several ion channels, such as K channel and aquaporins (22, 23). This reentrant loop plays an important role in the function of the ion channels; its role in NGEP is yet to be determined.

To further verify our predicted model based on epitope insertion technology, we generated three mAbs against the three discrete hydrophilic loops. The results proved that the epitopes used for generating the antibodies were intracellular, as immunofluorescence performed using these antibodies detected NGEP once the cells were permeabilized, supporting our model based on HA epitope insertion.

We also found that NGEP is expressed as an N-glycosylated protein in mammalian cells. Using mutational analysis, we found two *N*-glycosylation sites in the fourth extracellular loop, indicating that this part of the protein is indeed localized extracellularly, which again verifies our topology model of NGEP. Protein *N*-glycosylation plays many different roles in biological processes (24), including protein synthesis and secretion. Glycosylation is also likely to provide additional recognition sites for protein receptors. More specifically, *N*-glycosylation is required for the activity of many enzymes (25). The exact role of glycosylation in NGEP is yet to be established.

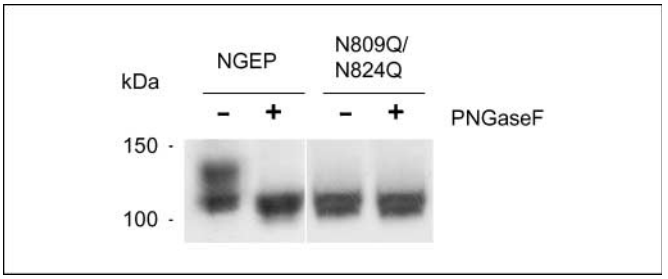

Figure 5. PNGaseF treatment of NGEP and *N*-glycosylation mutants of NGEP. Crude membrane fraction from MCF7/NGEP and N809Q/N824Q-NGEP/MCF7 was solubilized and treated with PNGaseF as described in Materials and Methods. Samples treated in parallel with (+) and without (−) PNGaseF were analyzed by Western blot using rabbit anti-NGEP polyclonal antibody. The shift in the mobility of wild-type NGEP seen after the treatment of PNGaseF disappeared after mutating the *N*-glycosylation sites.

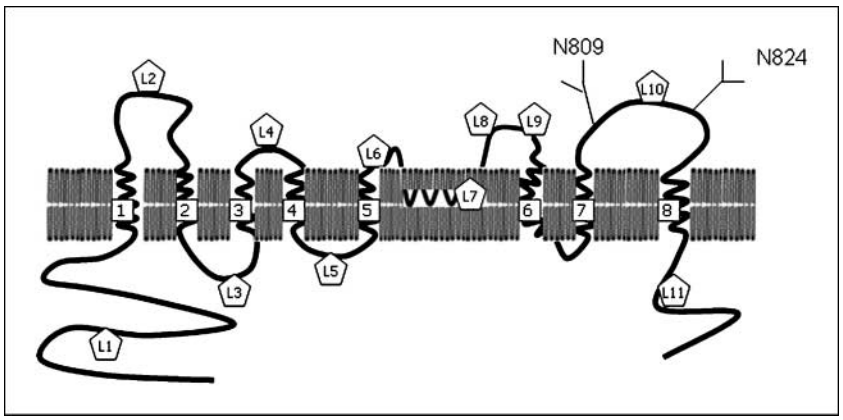

Figure 6. Model of NGEP topology. NGEP has eight transmembrane domains joined by hydrophilic loops. Both the NH_2 and COOH termini of NGEP are cytosolic. There is a reentrant loop between the transmembrane domains 5 and 6. The putative *N*-glycosylation sites N809 and N824 are shown.

We also showed that NGEP is expressed in primary prostate tumors and metastases, unlike prostate-specific membrane antigen, which apart from prostate is expressed in normal tissues such as kidney, liver, esophagus, stomach, small intestine, colon, brain, and lung (26, 27), and prostate stem cell antigen, which is overexpressed in prostate cancer but is also expressed in normal tissues such as esophagus, stomach, and kidney (28). Based on our RNA and immunohistochemical analysis, NGEP is only expressed in normal prostate (nonessential) and prostate cancer. This makes NGEP an excellent immunotherapeutic target and a mAb targeting an extracellular portion of NGEP could be useful in the immunotherapy of prostate cancer.

Understanding the topology structure of NGEP will help us to elucidate the structure-function relationship and help us further in the mechanistic interpretation of NGEP function. Identification of the putative extracellular regions of NGEP will be essential in guiding future work such as generating mAb to be tested for immunotherapeutic potential against prostate cancer.

Disclosure of Potential Conflicts of Interest

No potential conflicts of interest were disclosed.

Acknowledgments

Received 3/6/2008; revised 5/15/2008; accepted 5/28/2008.

Grant support: Intramural Research Program of the NIH, National Cancer Institute, Center for Cancer Research.

The costs of publication of this article were defrayed in part by the payment of page charges. This article must therefore be hereby marked *advertisement* in accordance with 18 U.S.C. Section 1734 solely to indicate this fact.

We thank Itai Pashtan (Laboratory of Molecular Biology, National Cancer Institute) for technical assistance, Susan Garfield and Poonam Mannan (Center for Cancer Research Confocal Microscopy Core Facility, National Cancer Institute) for technical support, NIH Fellows Editorial Board for valuable comments, and Anna Mazzuca for editorial assistance.

References

1. Jemal A, Siegel R, Ward E, Murray T, Xu J, Thun MJ. Cancer statistics. CA Cancer J Clin 2007;57:43–66.
2. Eble JN, Sauter G, Epstein JL, Sesterhenn IA. Pathology and genetics: tumors of the urinary system and male genital organs. Chapter 3. Lyon: IARC Press; 2004. p.10.
3. Messing EM, Manola J, Sarosdy M, Wilding G, Crawford ED, Trump D. Immediate hormonal therapy compared with observation after radical prostatectomy and pelvic lymphadenectomy in men with node-positive prostate cancer. N Engl J Med 1999;341:1781–8.
4. Pilepich MV, Winter K, John MJ, et al. Phase III radiation therapy oncology group (RTOG) trial 86-10 of androgen deprivation adjuvant to definitive radiotherapy in locally advanced carcinoma of the prostate. Int J Radiat Oncol Biol Phys 2001;50:1243–52.
5. Bolla M, Gonzalez D, Warde P, et al. Improved survival in patients with locally advanced prostate cancer treated with radiotherapy and goserelin. N Engl J Med 1997;337:295–300.
6. Stewart AJ, Scher HI, Chen MH, et al. Prostate-specific antigen nadir and cancer-specific mortality following hormonal therapy for prostate-specific antigen failure. J Clin Oncol 2005;23:6556–60.
7. Reichert JM, Rosensweig CJ, Faden LB, Dewitz MC. Monoclonal antibody successes in the clinic. Nat Biotechnol 2005;23:1073–8.
8. Pastan I, Hassan R, Fitzgerald DJ, Kreitman RJ. Immunotoxin therapy of cancer. Nat Rev Cancer 2006; 6:559–65.
9. Bera TK, Das S, Maeda H, et al. NGEP, a gene encoding a membrane protein detected only in prostate cancer and normal prostate. Proc Natl Acad Sci U S A 2004;101: 3059–64.
10. Das S, Hahn Y, Nagata S, et al. NGEP, a prostate-specific plasma membrane protein that promotes the association of LNCaP cells. Cancer Res 2007;67:1594–601.
11. Kyte J, Doolittle RF. A simple method for displaying the hydropathic character of a protein. J Mol Biol 1982; 157:105–32.
12. Rost B, Yachdav G, Liu J. The predict protein server. Nucleic Acids Res 2004;32:W321–6.
13. Kast C, Canfield V, Levenson R, Gros P. Transmembrane organization of mouse P-glycoprotein determines by epitope insertion and immunofluorescence. J Biol Chem 1998;271:9240–8.
14. Shih TM, Goldin AL. Topology of the *Shaker* potassium channel probed with hydrophilic epitope insertions. J Cell Biol 1997;136:1037–45.
15. Milpetz F, Argos P, Persson B. TMAP: a new email and WWW service for membrane-protein structural predictions. Trends Biochem Sci 1995;20:204–5.
16. Chenna R, Sugawara H, Koike T, et al. Multiple sequence alignment with the Clustal series of programs. Nucleic Acids Res 2003;31:3497–500.
17. Gama L, Breitwieser GE. Generation of epitope-tagged proteins by inverse polymerase chain reaction mutagenesis. Methods Mol Biol 2002;182:77–83.
18. Ise T, Das S, Nagata S, et al. Expression of POTE protein in human testis detected by novel monoclonal antibodies. Biochem Biophys Res Commun 2008;365: 603–8.
19. Cordes FS, Bright JN, Sansom MS. Proline-induced distortions of transmembrane helices. J Mol Biol 2002; 323:951–60.
20. Yohannan S, Faham S, Yang D, Whitelegge JP, Bowie JU. The evolution of transmembrane helix kinks and the structural diversity of G protein-coupled receptors. Proc Natl Acad Sci U S A 2004;101:959–63.
21. Viklund H, Granseth E, Elofsson A. Structural classification and prediction of reentrant regions in α-helical transmembrane proteins: application to complete genomes. J Mol Biol 2006;361:591–603.
22. Grunewald M, Kanner BI. The accessibility of a novel reentrant loop of the glutamate transporter GLT-1 is restricted by its substrate. J Biol Chem 2000;275:9684–9.
23. Sansom MS, Law RJ. Membrane proteins: aquaporins—channels without ions. Curr Biol 2001;11:R71–3.
24. Roth J. Protein N-glycosylation along the secretory pathway: relationship to organelle topography and function, protein quality control, and cell interactions. Chem Rev 2002;102:285–303.
25. Nagai K, Ihara Y, Wada Y, Taniguchi N. N-glycosylation is requisite for the enzyme activity and Golgi retention of N-acetylglucosaminyltransferase III. Glycobiology 1997;7:769–76.
26. Mhawech-Fauceglia P, Zhang S, Terracciano L, et al. Prostate-specific membrane antigen (PSMA) protein expression in normal and neoplastic tissues and its sensitivity and specificity in prostate adenocarcinoma: an immunohistochemical study using multiple tumour tissue microarray technique. Histopathology 2007;50: 472–83.
27. Kinoshita Y, Kuratsukuri K, Landas S, et al. Expression of prostate-specific membrane antigen in normal and malignant human tissues. World J Surg 2006;30:628–36.
28. Bahrenberg G, Brauers A, Joost HG, Jakse G. Reduced expression of PSCA, a member of the LY-6 family of cell surface antigens, in bladder, esophagus, and stomach tumors. Biochem Biophys Res Commun 2000;275:783–8.

Topology of NGEP, a Prostate-Specific Cell:Cell Junction Protein Widely Expressed in Many Cancers of Different Grade Level

Sudipto Das, Yoonsoo Hahn, Dawn A. Walker, et al.

Cancer Res 2008;68:6306-6312.